Journal of Solid State Chemistry 294 (2021) 121898

Contents lists available at ScienceDirect

Journal of Solid State Chemistry

journal homepage: www.elsevier.com/locate/jssc

Crystal and electronic structure, thermochemical and photophysical properties of europium-silver sulfate monohydrate $AgEu(SO_4)_2{\cdot}H_2O$

Yuriy G. Denisenko [a,b,c,*], Alexander E. Sedykh [b,d], Maxim S. Molokeev [e,f,g], Aleksandr S. Oreshonkov [f,h], Aleksandr S. Aleksandrovsky [i,j], Alexander S. Krylov [h], Nikolay A. Khritokhin [a], Elena I. Sal'nikova [a,k], Oleg V. Andreev [a,l], Klaus Müller-Buschbaum [b,d]

[a] Institute of Chemistry, Tyumen State University, Tyumen, 625003, Russia
[b] Institute of Inorganic and Analytical Chemistry, Justus-Liebig-University of Giessen, Giessen, 35392, Germany
[c] Department of General and Special Chemistry, Industrial University of Tyumen, Tyumen, 625000, Russia
[d] Center for Materials Research (LaMa), Justus-Liebig-University of Giessen, Giessen, 35392, Germany
[e] Laboratory of Crystal Physics, Kirensky Institute of Physics, Federal Research Center KSC SB RAS, Krasnoyarsk, 660036, Russia
[f] Siberian Federal University, Krasnoyarsk, 660041, Russia
[g] Department of Physics, Far Eastern State Transport University, Khabarovsk, 680021, Russia
[h] Laboratory of Molecular Spectroscopy, Kirensky Institute of Physics Federal Research Center KSC SB RAS, Krasnoyarsk, 660036, Russia
[i] Laboratory of Coherent Optics, Kirensky Institute of Physics Federal Research Center KSC SB RAS, Krasnoyarsk, 660036, Russia
[j] Institute of Nanotechnology, Spectroscopy and Quantum Chemistry, Siberian Federal University, Krasnoyarsk, 660041, Russia
[k] Komissarov Department of General Chemistry, Northen Trans-Ural Agricultural University, Tyumen, 625003, Russia
[l] Laboratory of the Chemistry of Rare Earth Compounds, Institute of Solid State Chemistry, UB RAS, Ekaterinburg, 620137, Russia

ARTICLE INFO

Keywords:
Structure
Thermochemistry
Luminescence
Sulfates
Europium

ABSTRACT

In order to synthesize single crystals of europium-silver double sulfate monohydrate, a hydrothermal reaction route was used. It was found that the crystallization cannot be performed under standard conditions. The compound $AgEu(SO_4)_2{\cdot}H_2O$ crystallizes in the trigonal crystal system, space group $P3_221$ (a = 6.917(1), c = 12.996(2) Å, V = 538.53(17) Å^3). The structure consists of triple-capped trigonal prisms [EuO_9], in which one oxygen atom belongs to crystalline water, silver octahedra [AgO_6], and sulfate tetrahedra [SO_4]. The hydrogen bonds in the system additionally stabilize the structure. The electronic band structure wasstudied by density functional theory calculations which show that $AgEu(SO_4)_2{\cdot}H_2O$ is an indirect band gap dielectric. Temperature dependent photoluminescence spectroscopy shows emission bands of transitions from the $^5D_0$ state to the spin-orbit components of the ^7F_Jmultiplet (J = 0–6).The ultranarrow transition $^5D_0$ - $^7F_0$ shows a red shift with respect to other europium-containing water-free sulfates that is ascribed to the presence of OH group in the crystal structure in the close vicinity of the Eu^{3+} ion. An effect of abnormal sensitivity of the Ω_4 intensity factor to minor distortions of the local environment is detected for the observed low local symmetry of C_2.

1. Introduction

Today, optical technologies determine progress in micro- and nanoelectronics, communication, processing, storage and display of information, medicine, biology, energy and other areas. One of the key areas of optics is photonics, which covers the field of science and technology associated with the use of light radiation in optical elements, devices, and systems in which optical signals are generated, amplified, and detected, as well as recorded or displayed [1–3]. The growing requirements for the quality of single-crystal materials associated with solving the problem of stabilizing the characteristics of optical devices require the development of methods for growing crystals with certain properties [4–7].

Recently, interest in rare-earth sulfates based materials has increased significantly, as they were found to be catalysts [8], phosphors [9–11], and gas adsorbents [12,13]. The decisive aspect of their application includes questions, such as polymorphism, isomorphism, and crystal-chemical transformations in the technological process [8–13].

Stoichiometric europium compounds are increasingly attracting attention of researchers due to the possibility of creating self-activated phosphors [14–18]. In contrast to doped phosphors, the uniqueness of

* Corresponding author. Institute of Chemistry, Tyumen State University, Tyumen, 625003, Russia.
E-mail address: yu.g.denisenko@gmail.com (Y.G. Denisenko).

https://doi.org/10.1016/j.jssc.2020.121898
Received 16 November 2020; Accepted 29 November 2020
Available online 11 December 2020

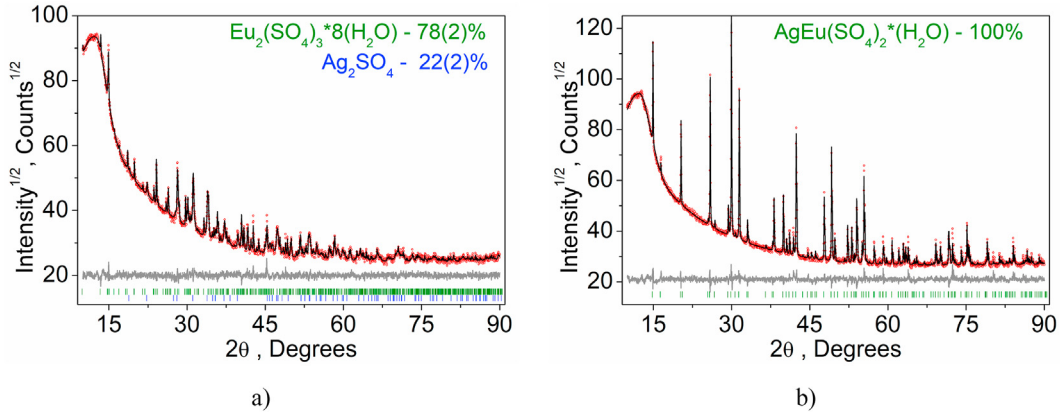

Fig. 1. Diffraction patterns of samples obtained by the crystallization of solutions containing stoichiometric amounts of Ag^{+}, Eu^{3+}, SO_4^{2-} (1:1:2) ions under normal (a) and hydrothermal (b) conditions.

Table 1
Crystal structure parameters of $AgEu(SO_4)_2{\cdot}H_2O$.

Single crystal	$AgEu(SO_4)_2{\cdot}H_2O$
Moiety formula	$AgEuH_2O_9S_2$
Dimension (mm)	0.3 × 0.25 × 0.2
Color	colourless
Molecular weight	469.97
Temperature (K)	296
Space group, *Z*	$P3_221$, 3
a (Å)	6.917 (1)
c (Å)	12.996 (2)
V (Å^3)	538.53 (17)
ρ_{calc} (g/cm^3)	4.347
μ (mm^{-1})	11.987
Reflections measured	11573
Reflections independent	1998
Reflections with $F > 4\sigma(F)$	1962
$2\theta_{max}$ (°)	78.06
h, *k*, *l*- limits	$-11 \le h \le 12$;$-11 \le k \le 12$;$-22 \le l \le 22$
R_{int}	0.0383
The weighed refinement of F^2	$w = 1/[\sigma^2(F_o^2)+(0.017P)^2+1.74P]$, $P = (F_o^2+2F_c^2)/3$
Number of refinement parameters	66
$R1$ [$F_o > 4\sigma(F_o)$]	0.0248
w$R2$	0.0552
Goof	1.128
$\Delta\rho_{max}$ (e/Å^3)	2.21
$\Delta\rho_{min}$ (e/Å^3)	−4.44
$(\Delta/\sigma)_{max}$	0.000

the crystallographic positions of the europium ions in such materials allows tracking of the influence non-structural factors on the luminescent properties [19–21].

Double salts of rare-earth elements also play a significant role for the technology of separation of rare-earth raw materials [22–27]. Moreover, double sulfates of rare-earth elements are of interest because of catalytic properties in redox processes [28,29]. The information on double sulfates containing trivalent europium is extremely episodic, while the corresponding double molybdates and europium tungstates with monovalent cations are well studied [30–33]. Employment of silver ions instead of alkaline ones in the structure of rare-earth containing double salts is expected to result in both variation of local field upon rare earth ions and variation of a complex of physical properties of a material that are important for some applications [34]. For the europium containing double sulfate monohydrates of potassium and thallium, the significant influence of reaction conditions and hydrothermal conditions is known [35–37].

The aim of this work is to study the crystallization conditions of europium-silver sulfate monohydrate from aqueous solutions, as well as to study its structural, thermochemical and luminescent properties.

2. Methods and materials

A crystallization base solution was prepared by mixing the three stock aqueous solutions: 5 ml $AgNO_3$ ($C(Ag^{+})$ = 1 mol/L), 5 ml $Eu(NO_3)_3$ ($C(Eu^{3+})$ = 1 mol/L), 5 ml H_2SO_4 ($C(SO_4^{2-})$ = 2 mol/L). Thus, a stoichiometric ion ratio was achieved in the base solution: Ag^{+}, Eu^{3+}, SO_4^{2-} (1:1:2). Methods for preparing stock solutions are given in the Supporting Information.

The crystallization from the base solution with a molar ratio of $1Ag^{+}$:$1Eu^{3+}$:$2SO_4^{2-}$ ions was carried out under two different conditions. In the first case, the base solution was left in a desiccator over concentrated sulfuric acid for 12 h (298K, 101325 Pa). In the second case, the hydrothermal crystallization was performed. For this, the base solution was transferred into a Teflon autoclave with a steel body and heated to a temperature of 180 °C. At this temperature, the autoclave was kept for 12 h. In both cases, the crystals formed were separated from the mother liquor on a Schott funnel, washed with deionized water, squeezed between sheets of filter paper and kept in a desiccator above water to a constant weight (~36 h).

The X-ray diffraction intensity patterns were collected from a single crystal of $AgEu(SO_4)_2{\cdot}H_2O$ at 23°C using a SMART APEX II single crystal diffractometer (Bruker AXS) equipped with a CCD-detector, graphite monochromator and MoKα radiation source. The absorption corrections were applied using the SADABS program. Absorption corrections were applied using the SADABS program. The crystal structures were solved by the direct methods using package SHELXS and refined in ananisotropic approach for all non-hydrogen atoms using the SHELXL program [37,38]. All hydrogen atoms of the H_2O molecules were found via Fourier difference maps and refined with bond length restraints d(O–H) = 0.9 Å and $U_{iso}(H) = 1.2U_{eq}(O)$.The structure test for the presence of missing symmetry elements and possible voids was produced using the program PLATON [39]. The program DIAMOND wasused for the crystal structure plotting [40].

The crystallographic data have been deposited in the Cambridge Crystallographic Data Centre (CCDC #2015507). The data can be downloaded from the site (www.ccdc.cam.ac.uk/data_request/cif).

For general phase analysis, X-ray powder diffraction was carried out on a BRUKER D2 PHASER diffractometer with a LYNXEYE linear detector (CuKα radiation, Ni filter). The higher quality powder X-ray diffraction data of $AgEu(SO_4)_2{\cdot}H_2O$ was obtained using a D8 ADVANCE diffractometer (Bruker) equipped by a VANTEC detector with a Ni filter. The measurements were made using Cu Kα radiation. The structural parameters defined by single crystal analysis were used as a base set for the

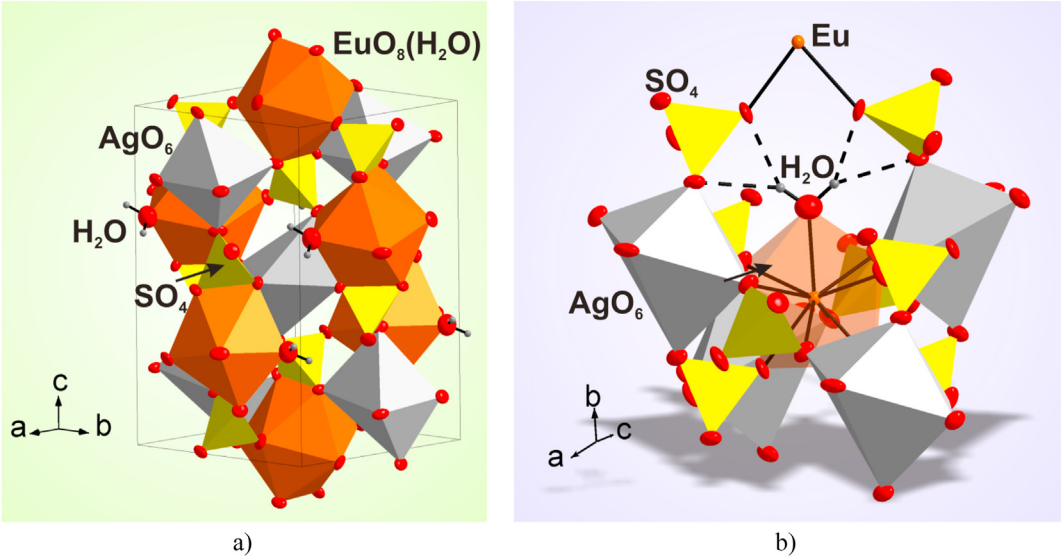

Fig. 2. Crystal structure of the $AgEu(SO_4)_2{\cdot}H_2O$ unit cell (a). The ellipsoids are drawn at the 80% probability level. Hydrogen bonds between H_2O molecule and SO_4^{2-} are depicted as dashed lines (b).

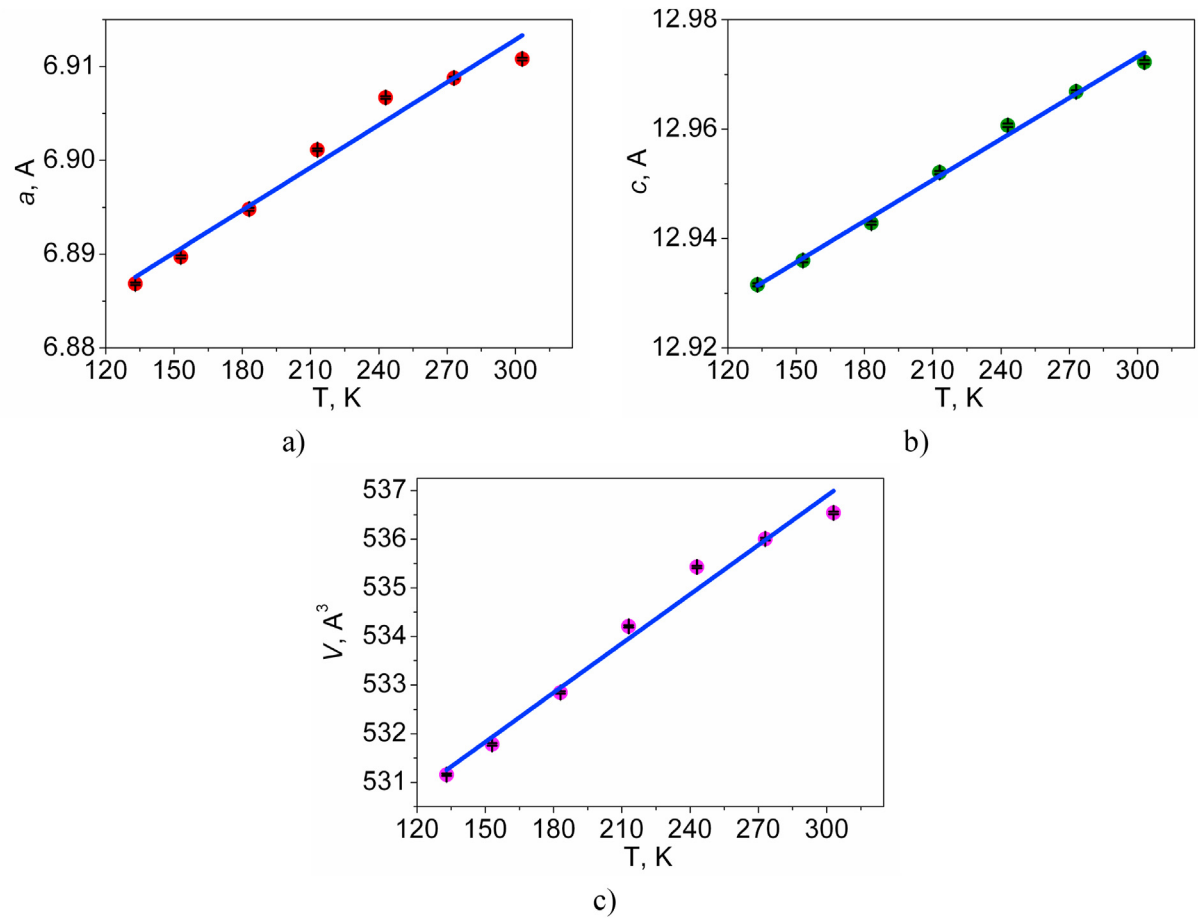

Fig. 3. Linear cell parameters increasing with T increasing: a) *a*(T); b) *c*(T); c) *V*(T).

Rietveld refinement of the powder pattern. The refinement was carried out using the program TOPAS 4.2 [41]. The low R-factors and good refinement results (Fig. 1S and Table 1S) indicate that the single crystal structure is representative also for the $AgEu(SO_4)_2{\cdot}H_2O$ bulk powder material.

Additional powder patterns were obtained under cooling in the range of 133–303K (Fig. 2S). The Le Bail fitting was used to obtain temperature-dependent cell parameters (Table 4S).

First-principle spin-polarized electronic structure calculations were carried out using the plane–wave pseudopotential approach (CASTEP

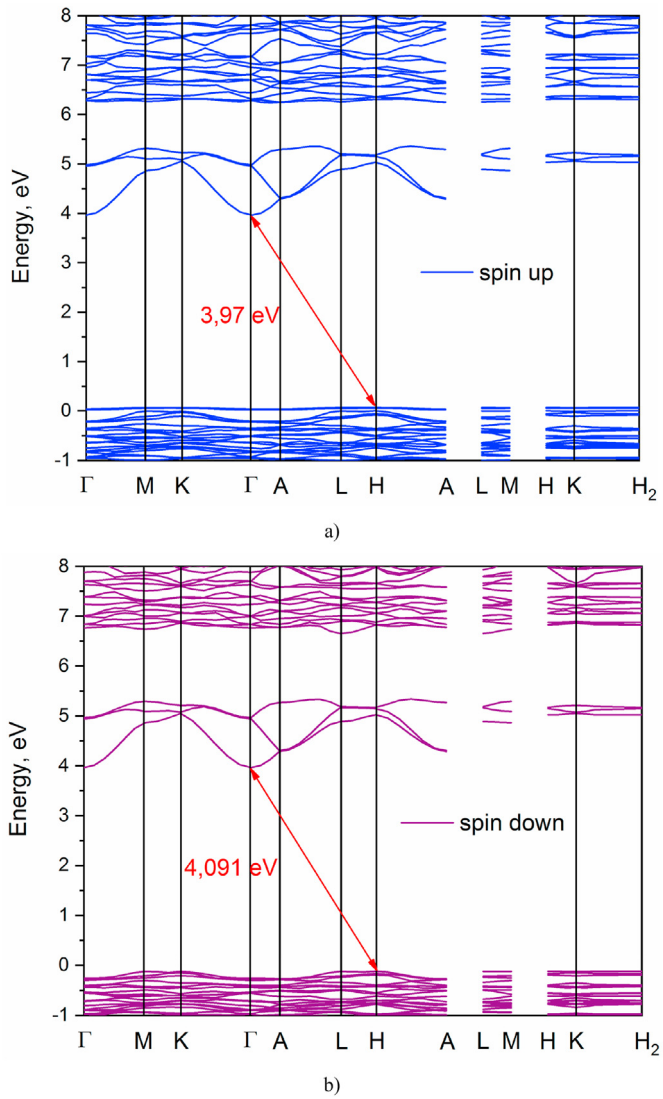

Fig. 4. Electronic band structure of $AgEu(SO_4)_2{\cdot}H_2O$: (a) - spin up, (b) – spin down.

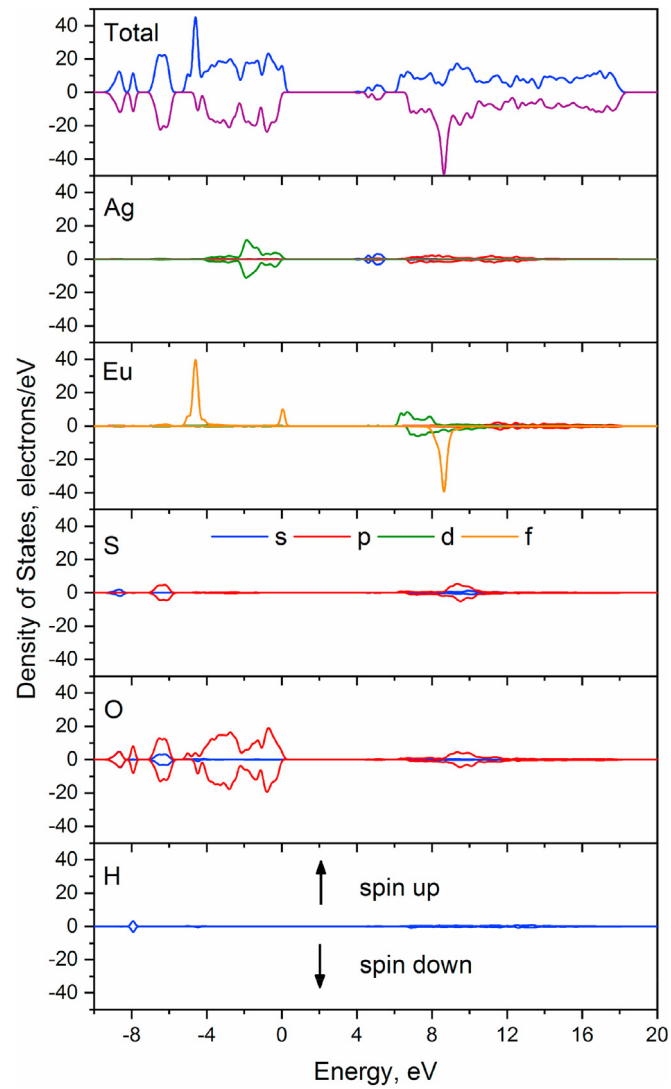

Fig. 5. Total and partial densities of states of $AgEu(SO_4)_2{\cdot}H_2O$.

package [42]), and the Perdew-Burke-Emzerhof (PBE) [43] functional within generalized gradient approximation (GGA) [44] was chosen to describe the exchange-correlation functional. The Hubbard U energy term U_f [45] = 6 eV for the Eu 4f orbital was used. Ultrasoft pseudopotentials generated on-the-fly in CASTEP code were used for calculation and include $4s^2\ 4p^6\ 4d^{10}\ 5s^1$ electrons for Ag, $4f^7 5s^2 5p^6 6s^2$ electrons for Eu, $3s^2 3p^4$ electrons for S, $2s^2 2p^4$ electrons for O and $1s^1$ electrons for H as valence ones. The self-consistent field (SCF) tolerance was set to 1.0×10^{-7} eV/atom. An energy cutoff of 630 eV was used with $3 \times 3 \times 2$ sampling of the Brillouin zone (BZ) using the Monkhorst–Pack scheme [46].

Fourier-transformed infrared spectroscopy (FTIR) was carried out with a Fourier Transform Infrared Spectrometer FSM 1201 (Infraspec, Russia). The sample for the investigation was prepared in the form of a tabletby addition of annealed KBr.

Thermal analysis was carried out by simultaneous differential thermal analysis and thermogravimetry on a thermal analysis instrument (STA equipment 499 F5 Jupiter NETZSCH (Germany). The powder samples were inserted into alumina crucibles and heated with a heating rate of 3°C/min from room temperature to 1300 °C. For heat flow change determination, the equipment was calibrated with standard substances, such as In, Sn, Bi, Zn, Al, Ag, Au, Ni, prior to the investigation, and the

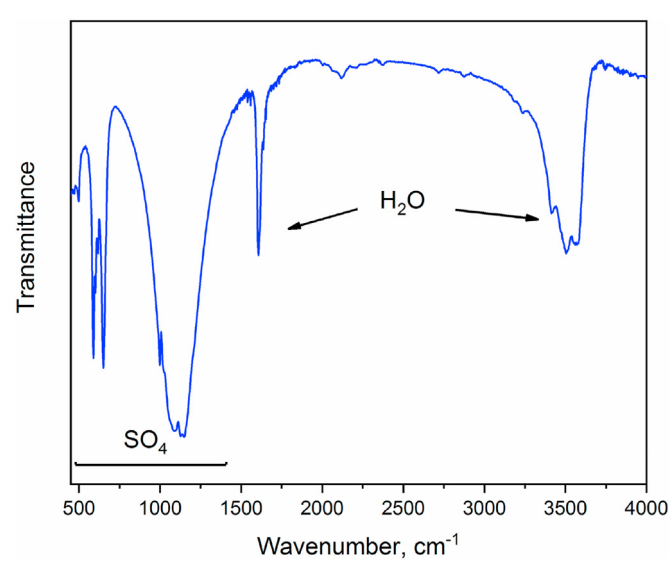

Fig. 6. Infrared spectrum of $AgEu(SO_4)_2{\cdot}H_2O$ obtained at room temperature.

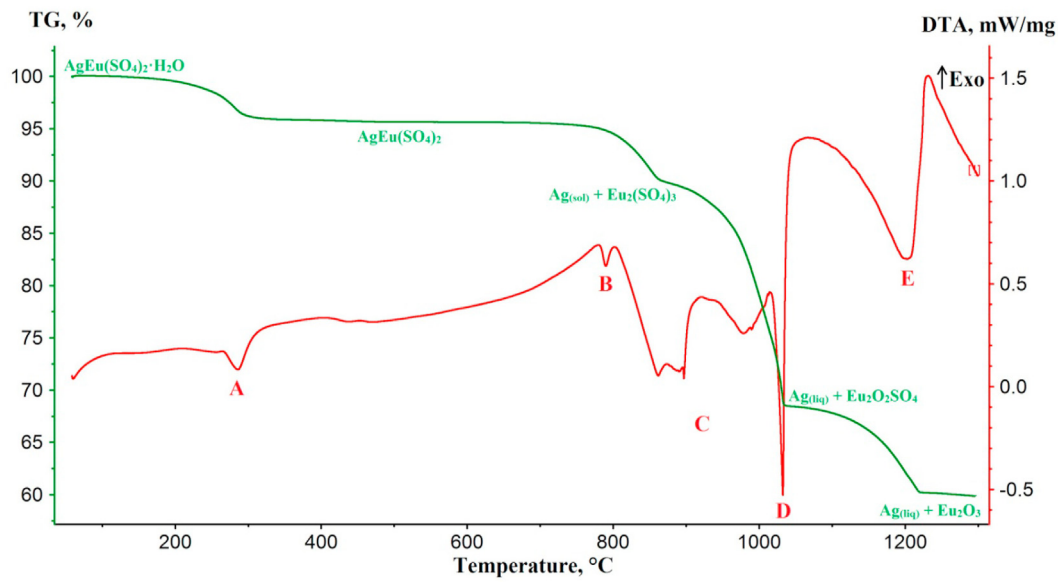

Fig. 7. Simultaneous TG/DTA of $AgEu(SO_4)_2{\cdot}H_2O$.

Table 2
Thermal effects upon decomposition of $AgEu(SO_4)_2{\cdot}H_2O$.

Thermal effect	Reaction	Ref.
A	$AgEu(SO_4)_2{\cdot}H_2O \rightarrow AgEu(SO_4)_2 + H_2O$	This work
B	$2AgEu(SO_4)_2 \rightarrow 2Ag + Eu_2(SO_4)_3 + SO_2 + O_2$	[17]
C	$Eu_2(SO_4)_3 \rightarrow Eu_2O_2SO_4 + 2SO_2 + O_2$	[46]
D	$Ag_{(sol)} \rightarrow Ag_{(liq)}$	[47]
E	$Eu_2O_2SO_4 \rightarrow Eu_2O_3 + SO_2 + {}^1/_2O_2$	[46]

results were analyzed with the program package Proteus 6 2012.

For the photoluminescence investigations, the sample was mortared, filled in a quartz glass cuvette, and examined at room temperature and at 77 K (using special liquid nitrogen-filled Dewar assembly). The spectra were recorded with a Horiba Jobin Yvon Spex Fluorolog 3 spectrophotometer equipped with a 450 W Xe short-arc lamp (USHIO), a 10 W xenon flash lamp (Excelitas FX-1102), double-grated excitation and emission monochromators, a photomultiplier tube (R928P) and a TCSPC upgrade using the FluoroEssence software. Both excitation and emission spectra were corrected for the spectral response of the monochromators and detector using spectral corrections provided by the manufacturers. Also, the excitation spectra were corrected for the spectral distribution of the lamp intensity by use of a photodiode reference detector. The emission decays were recorded using the Data Station software. Exponential tail fitting was used for calculation of the resulting intensity decay using the Decay Analysis software. The quality of each fit was confirmed by χ^2 value.

3. Results and discussions

The conditions of crystallization from solutions containing stoichiometric amounts of Ag^+, Eu^{3+}, SO_4^{2-} (1:1:2) ions significantly affect the composition of the crystallized products. Thus, crystallization at room temperature and normal atmospheric pressure in the presence of a drying agent (H_2SO_4) leads to a mixture of separate single crystals of Ag_2SO_4 and $Eu_2(SO_4)_3{\cdot}8H_2O$ (Fig. 1a). At the same time, carrying out hydrothermal crystallization at a temperature of 180 °C and an elevated pressure created in a closed system (autoclave) allows one to obtain single crystals of europium-silver double sulfate monohydrate $AgEu(SO_4)_2{\cdot}H_2O$ (Fig. 1b). Transparent, shiny single crystals were obtained with a yield of 67.4% (1.5836 g).

The unit cell of $AgEu(SO_4)_2{\cdot}H_2O$ corresponds to trigonal symmetry. Space group $P3_221$ was determined from the statistical analysis of the reflection intensities and extinction rules. The main crystal data are shown in Table 1. The atom coordinates and main interatomic distances are given in Tables 2S and 3S, respectively. The asymmetric part of the unit cell contains one Eu^{3+} ion, one Ag^+ ion, one S^{6+} ion, four O^{2-} ion and one H_2O molecule. The Ag^+ ion is coordinated by six O^{2-} ions forming octahedra, S^{6+} ion coordinated by four O^{2-} ions forming tetrahedra and Eu^{3+} ion is coordinated by eight O^{2-} ions and one H_2O molecule forming tricapped trigonal prism (Fig. 2a). All polyhedra join with each other by nodes, forming a 3D net. The H_2O molecule has H-bonding with SO_4 ions (Fig. 2b) which additionally stabilize the structure.

According to the data of temperature dependent powder diffractometry, the compound has positive thermal expansion coefficients in all crystallographic directions in the temperature range of 133–303 K (Fig. 3). The crystals expand almost isotropically. Moreover, the crystals expand almost isotropically with thermal expansion because α(a), α(c) thermal expansion coefficients are similar: $\alpha(a) = 20.5 \times 10^{-6}$ 1/K; $\alpha(c) = 18.5 \times 10^{-6}$ 1/K. The cell volume also has positive thermal expansion $\alpha(V) = 59.6 \times 10^{-6}$ 1/K.

The path along Brillouin zone high-symmetry points was chosen as Γ-*M*-K-Γ-A-L-H-A|L-M|H–K–H_2 for the $AgEu(SO_4)_2{\cdot}H_2O$ electronic band structure calculations. Coordinates of these points are: Γ(0,0,0), M(0.5,0,0), K(0.3333,0.3333,0), A(0,0,0.5), L(0.5,0,0.5), H(0.3333,0.3333,0.5), H_2(0.3333,0.3333,-0.5). The calculated spin-polarized electronic band structure of $AgEu(SO_4)_2{\cdot}H_2O$ is presented in Fig. 4. It can be observed that the conduction band minimum (CBM) and valence band maximum (VBM) are found at the Γ and H points, correspondingly. Thus, the $AgEu(SO_4)_2 \times H_2O$ is an indirect band gap materials and values of E^i gareequal to 3.97 and 4.091 eV for spin up and spin down band gaps, respectively. The direct electronic transitions in $AgEu(SO_4)_2{\cdot}H_2O$ are in the vicinity of the Γ point. The band gap value of $AgEu(SO_4)_2{\cdot}H_2O$ was also obtained by the determination of fundamental absorption edge from the absorption spectrum as shown in Fig. 3S. The value of experimental optical band gap is about 4.56 eV. It should be noted, that according the results of calculation, the direct optical band gap is in the vicinity of Γ point and the difference between direct and indirect transitions is very small (~0.02 eV).

The total and partial density of states (DOS) of the $AgEu(SO_4)_2{\cdot}H_2O$ (Fig. 5) were calculated to explain the nature of the electronic band structure. The partial DOS of spin up and spin down of Ag, S, O, and H atoms are nearly symmetrical, while spin states of Eu atoms have

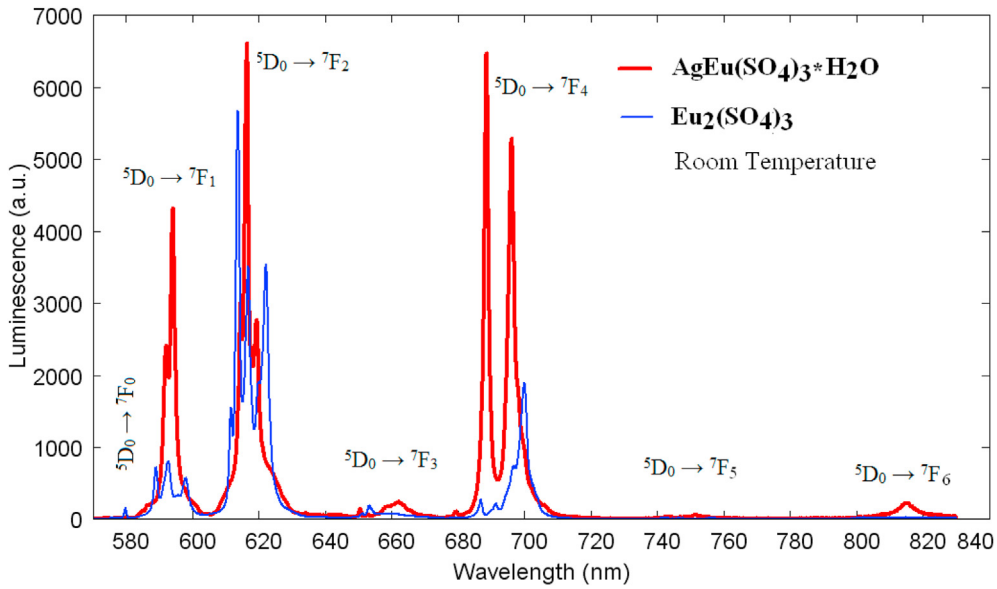

a)

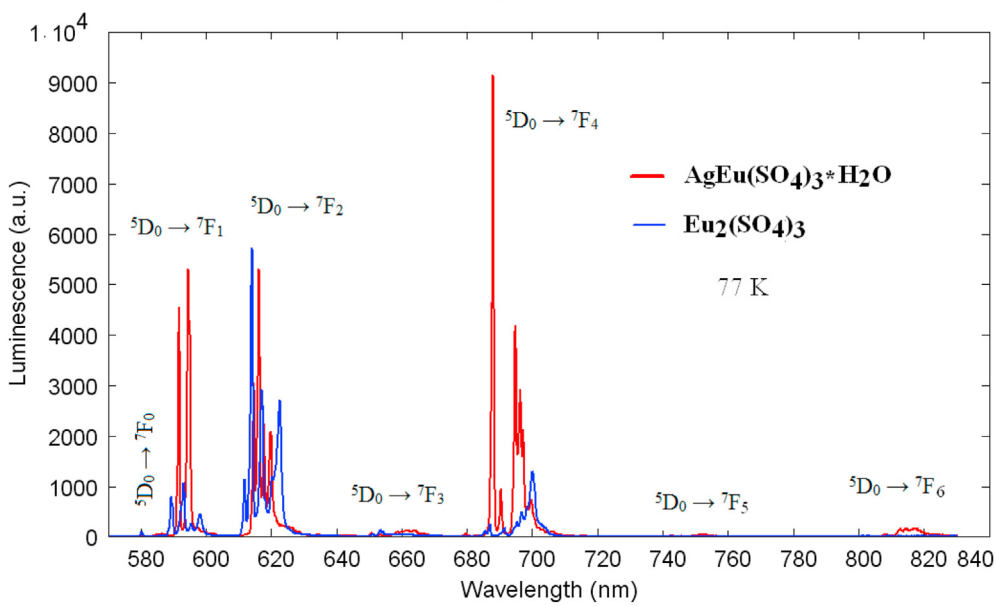

b)

Fig. 8. Emission spectra of $AgEu(SO_4)_2{\cdot}H_2O$ (red) and of a reference crystal $Eu_2(SO_4)_3$ (blue) at room temperature (a) and 77K (b). (For interpretation of the references to colour in this figure legend, the reader is referred to the Web version of this article.)

different patterns. It is clearly seen from Fig. 5, that 4d Ag, 4f Eu, and 2p O orbitals participate in the VBM hybridization. The band states between 4 and 5.5 eV originate from s electrons of Ag (CBM), but the contribution to the Total DOS of these electrons is weak. The higher valence bands (from 6 to 9.2 eV) are occupied by d and f electrons of Eu.

The infrared spectrum of $AgEu(SO_4)_2{\cdot}H_2O$ is presented in Fig. 6. According to the symmetry analysis of $P3_221$ space group, the vibrational representation at the Brillouin zone center should be written as $\Gamma_{vibr} = 21A_1 + 24A_2 + 45E$. The modes of symmetry A_2 (23 modes) are IR-active, while Raman-active modes are A_1 (21 modes). The E modes (44 modes) are active in both Infrared and Raman spectra. One A_2 and one E modes being acoustical. In the IR spectrum, the sulfate bands are located in the range of 500–1300 cm^{-1}. The internal symmetric and antisymmetric stretching vibrations of $[SO_4]^{2-}$ ions are situated between 990 and 1300 cm^{-1}. In Fig. 6, the spectral bands below 700 cm^{-1} represent bending modes of sulfate tetrahedra. The strong bands in high-wavenumber region of the spectra are vibrational modes of H_2O molecules. The symmetric and antisymmetric stretching modes are in the range of 3300–3650 cm^{-1} and region 1570-1670 $cm^{-1}$is related to bending modes.

The TG/DTA curves obtained for $AgEu(SO_4)_2{\cdot}H_2O$ in the temperature range of 50–1300 °C are presented in Fig. 7. A description of the processes occurring during thermal decomposition is systematized in Table 2. As can be seen, in the temperature range 100–300 °C, a weight loss is observed corresponding to complete dehydration of the monohydrate (peak A). Despite the fact that, according to the TG data, the dehydration occurs in one stage, a kink in the DTA curve suggests a

stepwise nature of the process. As a result, an anhydrous double sulfate of the potential composition $AgEu(SO_4)_2$ is formed, which is stable up to 700°C, after which it decomposes into metallic silver and europium sulfate (peak B) [17]. The further behavior of the sample is explained by the stepwise decomposition of europium sulfate $Eu_2(SO_4)_3$ (Peak group C), resulting in a mixture consisting of metallic silver and europium oxysulfate [17,47]. Peak D corresponds to the melting of metallic silver [48]. The strong peak E corresponds to the decomposition of europium oxysulfate to the stable form of Eu_2O_3 [47].

In order to evaluate the photoluminescence (PL) properties, emission and excitation spectra were recorded at room temperature and 77 K and determined the overall process decay times of the PL processes. The overall room-temperature luminescence spectrum of $AgEu(SO_4)_2{\cdot}H_2O$ excited at 393 nm is plotted in Fig. 8a in comparison with that from a reference crystal (anhydrous europium sulfate $Eu_2(SO_4)_3$) [16]. Both spectra contain emission bands related to the transitions from $^5D_0$ state to spin-orbit components of ^7F_J multiplet (J = 0–6). According to the results of XRD analysis (section XRD), Eu ions in the lattice of trigonal $AgEu(SO_4)_2{\cdot}H_2O$ occupy a single inequivalent site and are coordinated by nine oxygen ions, just like in the reference crystal $Eu_2(SO_4)_3$. However, in the crystal under study, the violation of inversion symmetry is more weakly pronounced. As the result, in $AgEu(SO_4)_2{\cdot}H_2O$, the intensities of magnetic dipole band $^5D_0$ - $^7F_1$ and hypersensitive band $^5D_0$ - $^7F_2$ are approximately the same while in the reference crystal the hypersensitive band evidently dominates. The local symmetry of the Eu ion in trigonal $AgEu(SO_4)_2{\cdot}H_2O$ is C_2, while in the reference monoclinic crystal $Eu_2(SO_4)_3$, the local symmetry is C_1. Therefore, the ultranarrow transition $^5D_0 \rightarrow {}^7F_0$must be observed in both crystals. However, we established that the peak amplitude for $^5D_0 \rightarrow {}^7F_0$in $AgEu(SO_4)_2{\cdot}H_2O$ is much smaller in comparison with the magnetic dipole band transition$^5D_0 \rightarrow {}^7F_1$ than in $Eu_2(SO_4)_3$. This means that the violation of mirror symmetry at the Eu site in $AgEu(SO_4)_2{\cdot}H_2O$ is considerably weaker than in $Eu_2(SO_4)_3$. The position of the ultranarrow peak in $AgEu(SO_4)_2{\cdot}H_2O$ is 580.5 nm, while in anhydrous triclinic $AgEu(SO_4)_2$ [17], it is blue-shifted to 578.5 nm, and in Ag-free $Eu_2(SO_4)_3$ it is detected at 580 nm. Therefore, we must note that the inclusion of water molecules into the crystal structure resulted in a rather unexpected red shift of position of ultranarrow transition. The Eu^{3+} emission lifetime of $AgEu(SO_4)_2{\cdot}H_2O$ is slightly shorter than the typical ones for inorganic and coordination compounds (0.8–4 ms) [49–53] and is 0.4603(3)ms. This is due to the water molecule that entered the crystal structure in close vicinity of Eu^{3+} and it provided non-radiative relaxation of excited state by O–H bond vibrations.

The overall 77 K luminescence spectrum of $AgEu(SO_4)_2{\cdot}H_2O$ excited at 393 nm is plotted in Fig. 8b in comparison with that of a reference crystal (anhydrous europium sulfate $Eu_2(SO_4)_3$ [16]). A remarkable feature of the $AgEu(SO_4)_2{\cdot}H_2O$ luminescence is the high intensity of $^5D_0 \rightarrow {}^7F_4$ band that is especially pronounced at 77 K. This feature was observed earlier [54] and was explained by the interplay of minor distortions from D_{4d} local symmetry of Eu^{3+} ion in a highly polarizable environment. It is highly likely that $AgEu(SO_4)_2{\cdot}H_2O$ is an example of a crystal structure with the manifestation of the same effect for a lower local symmetry. This crystal structure enables a higher value of the Ω_4 intensity parameter with respect to $Eu_2(SO_4)_3$ and, moreover, a variation of interionic distances upon cooling reveals high sensitivity of this effect to sequent minor variations of the amplitudes of components of crystal field. This explanation is supported by the fact that the internal substructure of $^5D_0 \rightarrow {}^7F_4$ experiences maximum restructuration upon cooling in comparison with the restructuration of other bands. Upon cooling down to 77 K, the Eu^{3+} emission lifetime of $AgEu(SO_4)_2{\cdot}H_2O$ rises to 0.7040(5)ms, as the luminescence quenching by O–H bonds vibrations of coordinated water molecule decreases.

4. Conclusions

By hydrothermal crystallization, a monohydrate of europium-silver double sulfate was obtained. The close relationship with the structures of the previously described compounds $AEu(SO_4)_2{\cdot}H_2O$ (A = K, Tl) allows us to suggest the possibility of the existence of polymorphic modifications. However, to systematize a number of $AEu(SO_4)_2{\cdot}H_2O$ structures (A = alkali metal, Cu, Ag, Au, Tl), at this stage there is insufficient data and work in this direction should be continued. Data on the characterization of the compound by various methods allow itto be considered as a multifunctional material. The compound exhibits excellent luminescent filaments and can be considered as a self-activated red phosphor. First principle calculations of the electronic band structure revealed that $AgEu(SO_4)_2{\cdot}H_2O$ is an indirect band gap material. As a result, the properties of the material can significantly depend on temperature. In addition to the properties described in this paper, the present framework structure can also be considered in the catalysis of various organic reactions.

Declaration of competing interest

The authors declare that they have no known competing financial interests or personal relationships that could have appeared to influence the work reported in this paper.

Acknowledgement

This work was partially supported by the Russian Foundation for Basic Research (Grant 19-33-90258\19). Use of equipment of Krasnoyarsk Regional Center of Research Equipment of Federal Research Center « Krasnoyarsk Science Center SB RAS» is acknowledged.

Appendix A. Supplementary data

Supplementary data to this article can be found online at https://doi.org/10.1016/j.jssc.2020.121898.

References

[1] D.L. Andrews, Photon-based and classical descriptions in nanophotonics: a review, J. Nanophotonics 8 (2014), 081599.
[2] E. Khalkhal, M. Rezaei-Tavirani, M.R. Zali, Z. Akbari, The evaluation of laser application in surgery: a review article, J. Laser Med. Sci. 10 (2019) S104–S111.
[3] A. Leung, P.M. Shankar, R. Mutharasan, A review of fiber-optic biosensors, Sensor. Actuator. B Chem. 125 (2007) 688–703.
[4] A. Kuramata, K. Koshi, S. Watanabe, Y. Yamaoka, T. Masui, S. Yamakoshi, High-quality β-Ga_2O_3 single crystals grown by edge-defined film-fed growth, Jpn. J. Appl. Phys. 55 (2016) 1202A2.
[5] Y. Liu, Y. Zhang, K. Zhao, Z. Yang, J. Feng, X. Zhang, K. Wang, L. Meng, H. Ye, M. Liu, S. Liu, A 1300 mm^2 ultrahigh-performance digital imaging assembly using high-quality perovskite single crystals, Adv. Mater. 30 (2018) 1707314.
[6] Y. Liu, Y. Zhang, Z. Yang, J. Feng, Z. Xu, Q. Li, M. Hu, H. Ye, X. Zhang, M. Liu, K. Zhao, S. Liu, Low-temperature-gradient crystallization for multi-inch high-quality perovskite single crystals for record performance photodetectors, *mater*, Today Off. 22 (2019) 67–75.
[7] F. Ye, H. Lin, H. Wu, L. Zhu, Z. Huang, D. Ouyang, G. Niu, W.C.H. Choy, High-quality cuboid $CH_3NH_3PbI_3$ single crystals for high performance X-ray and photon detectors, Adv. Funct. Mater. 29 (2019) 1806984.
[8] C. Cascales, B.G. Lor, E.G. Puebla, M. Iglesias, M.A. Monge, C.R. Valero, N. Snejko, Catalytic behavior of rare-earth sulfates: applications in organic hydrogenation and oxidation reactions, Chem. Mater. 16 (2004) 4144–4149.
[9] T. Kijima, T. Shinbori, M. Sekita, M. Uota, G. Sakai, Abnormally enhanced Eu^{3+} emission in $Y_2O_2SO_4$:Eu^{3+} inherited from their precursory dodecylsulfate-templated concentric-layered nanostructure, J. Lumin. 128 (2008) 311–316.
[10] T. Kijima, T. Isayama, M. Sekita, M. Uota, G. Sakai, Emission properties of Tb^{3+} in $Y_2O_2SO_4$ derived from their precursory dodecylsulfate-templated concentric- and straight-layered nanostructures, J. Alloys Compd. 485 (2009) 730–733.
[11] G.L. Sharipov, A.A. Tukhbatullin, A.M. Abdrakhmanov, Triboluminescence of crystals and suspensions of inorganic salts of lanthanides, Protect. Met. Phys. Chem. Surface 47 (2011) 13–19.
[12] D. Zhang, T. Kawada, F. Yoshioka, M. Machida, Oxygen gateway effect of CeO_2/$La_2O_2SO_4$ composite oxygen storage materials, ACS Omega 1 (2016) 789–798.
[13] W. Zhang, I.W.C.E. Arends, K. Djanashvili, Nanoparticles of lanthanide oxysulfate/oxysulfide for improved oxygen storage/release, Dalton Trans. 45 (2016) 14019–14022.
[14] Yu G. Denisenko, M.S. Molokeev, A.S. Krylov, A.S. Aleksandrovsky, A.S. Oreshonkov, V.V. Atuchin, N.O. Azarapin, P.E. Plyusnin, E.I. Sal'nikova, O.V. Andreev, High-temperature oxidation of europium (II) sulfide, J. Ind. Eng. Chem. 79 (2019) 62–70.

[15] V.V. Atuchin, A.S. Aleksandrovsky, B.G. Bazarov, J.G. Bazarova, O.D. Chimitova, Yu G. Denisenko, T.A. Gavrilova, A.S. Krylov, E.A. Maximovskiy, M.S. Molokeev, A.S. Oreshonkov, A.M. Pugachev, N.V. Surovtsev, Exploration of structural, vibrational and spectroscopic properties of self-activated orthorhombic double molybdate $RbEu(MoO_4)_2$ with isolated MoO_4 units, J. Alloys Compd. 785 (2019) 692–697.

[16] Yu G. Denisenko, A.S. Aleksandrovsky, V.V. Atuchin, A.S. Krylov, M.S. Molokeev, A.S. Oreshonkov, N.P. Shestakov, O.V. Andreev, Exploration of structural, thermal and spectroscopic properties of self-activated sulfate $Eu_2(SO_4)_3$ with isolated SO_4 groups, J. Ind. Eng. Chem. 68 (2018) 109–116.

[17] Yu G. Denisenko, V.V. Atuchin, M.S. Molokeev, A.S. Aleksandrovsky, A.S. Krylov, A.S. Oreshonkov, S.S. Volkova, O.V. Andreev, Structure, thermal stability, and spectroscopic properties of triclinic double sulfate $AgEu(SO_4)_2$ with isolated SO_4 groups, Inorg. Chem. 57 (2018) 13279–13288.

[18] Yu G. Denisenko, N.O. Azarapin, N.A. Khritokhin, O.V. Andreev, S.S. Volkova, Europium oxysulfate $Eu_2O_2SO_4$ crystal structure, Russ. J. Inorg. Chem. 64 (2019) 7–12.

[19] V.V. Atuchin, A.S. Aleksandrovsky, O.D. Chimitova, T.A. Gavrilova, A.S. Krylov, M.S. Molokeev, A.S. Oreshonkov, B.G. Bazarov, J.G. Bazarova, Synthesis and spectroscopic properties of monoclinic α-$Eu_2(MoO_4)_3$, J. Phys. Chem. C 118 (2014) 15404–15411.

[20] H. Ji, Z. Huang, Z. Xia, M.S. Molokeev, X. Jiang, Z. Lin, V.V. Atuchin, Comparative investigations of the crystal structure and photoluminescence property of eulytite-type $Ba_3Eu(PO_4)_3$ and $Sr_3Eu(PO_4)_3$, *dalt*, OR Trans. 44 (2015) 7679–7686.

[21] A.H. Reshak, Z.A. Alahmed, J. Bila, V.V. Atuchin, B.G. Bazarov, O.D. Chimitova, M.S. Molokeev, I.P. Prosvirin, A.P. Yelisseyev, Exploration of the electronic structure of monoclinic α-$Eu_2(MoO_4)_3$: DFT-based study and X-ray photoelectron spectroscopy, J. Phys. Chem. C 120 (2016) 10559–10568.

[22] M. Kul, Y. Topkaya, İ. Karakaya, Rare earth double sulfates from pre-concentrated bastnasite, Hydrometallurgy 93 (2008) 129–135.

[23] T. Jun, Y. Jingqun, C. Ruan, R. Guohua, J. Mintao, O. Kexian, Kinetics on leaching rare earth from the weathered crust elution-deposited rare earth ores with ammonium sulfate solution, Hydrometallurgy 101 (2010) 166–170.

[24] D. Beltrami, G.J.P. Deblonde, S. Bélair, V. Weigel, Recovery of yttrium and lanthanides from sulfate solutions with high concentration of iron and low rare earth content, Hydrometallurgy 157 (2015) 356–362.

[25] Z. Zhu, Y. Pranolo, C.Y. Cheng, Separation of uranium and thorium from rare earths for rare earth production – a review, Miner. Eng. 77 (2015) 185–196.

[26] M.K. Jha, A. Kumari, R. Panda, J. Rajesh Kumar, K. Yoo, J.Y. Lee, Review on hydrometallurgical recovery of rare earth metals, Hydrometallurgy 165 (2016) 2–26.

[27] J. Cui, L. Zhang, Metallurgical recovery of metals from electronic waste: a review, J. Hazard Mater. 158 (2008) 228–256.

[28] J. Perles, C. Fortes-Revilla, E. Gutiérrez-Puebla, M. Iglesias, M.Á. Monge, C. Ruiz-Valero, N. Snejko, Synthesis, structure, and catalytic properties of rare-earth ternary sulfates, Chem. Mater. 17 (2005) 2701–2706.

[29] Z. Deng, F. Bai, Y. Xing, N. Xing, L. Xu, Reaction in situ found in the synthesis of a series of lanthanide sulfate complexes and investigation on their structure, spectra and catalytic activity, Open J. Inorg. Chem. (2013) 76–99, 03.

[30] Z. Wang, H. Liang, M. Gong, Q. Su, The red phosphor $NaEu(MoO_4)_2$ prepared by the combustion method, Mater. Lett. 62 (2008) 619–622.

[31] C. Guo, S. Wang, T. Chen, L. Luan, Y. Xu, Preparation of phosphors $AEu(MoO_4)_2$ (A = Li, Na, K and Ag) by sol-gel method, Appl. Phys. A 94 (2009) 365–371.

[32] H. Yamamoto, S. Seki, T. Ishiba, The Eu site symmetry in $AEu(MoO_4)_2$ (A = Cs or Rb) generating saturated red luminescence, J. Solid State Chem. 94 (1991) 396–403.

[33] J. Huang, J. Xu, H. Luo, X. Yu, Y. Li, Effect of alkali-metal ions on the local structure and luminescence for double tungstate compounds $AEu(WO_4)_2$ (A = Li, Na, K), Inorg. Chem. 50 (2011) 11487–11492.

[34] C. You, L. Yue, C. Colón, F. Fernández-Martínez, L. Lin, M. Gao, Characterization and photoluminescence properties of $AgLn(MoO_4)(WO_4)$: novel silver based scheelite-type compounds, J. Lumin. 210 (2019) 255–260.

[35] K. Kazmierczak, H.A. Höppe, Syntheses, Crystal structures and vibrational spectra of $KLn(SO_4)_2{\cdot}H_2O$ (Ln=La, Nd, Sm, Eu, Gd, Dy), J. Solid State Chem. 183 (2010) 2087–2094.

[36] A.K. Paul, Synthesis and crystal structure of a new polymorph of potassium europium (III) bis(sulfate) monohydrate, $KEu(SO_4)_2{\cdot}H_2O$, Acta Crystallogr. Sect. E Crystallogr. Commun. 74 (2018) 242–245.

[37] P.N. Iyer, K.D. Singh Mudher, N.K. Kulkarni, Preparation and characterisation of $TlLn(SO_4)_2{\cdot}H_2O$ (Ln=Sm to Lu, Y), J. Alloys Compd. 252 (1997) 71–75.

[38] G.M. Sheldrick, A short history of *SHELX*, ActaCrystallogr. Sect. A Found. Crystallogr. 64 (2008) 112–122.

[39] PLATON – A Multipurpose Crystallographic Tool, Utrecht University, Utrecht, The Netherlands, 2008.

[40] K. Brandenburg, M. Berndt, DIAMOND - visual crystal structure information system CRYSTAL IMPACT, Post 1251, D-53002 Bonn.

[41] Bruker AXS TOPAS V4: General Profile and Structure Analysis Software for Powder Diffraction Data. – User's Manual, Bruker AXS, Karlsruhe, Germany, 2008.

[42] S.J. Clark, M.D. Segall, C.J. Pickard, P.J. Hasnip, M.I.J. Probert, K. Refson, M.C. Payne, First principles methods using CASTEP, Z. für Kristallogr. - Cryst. Mater. 220 (2005) 576.

[43] J.P. Perdew, K. Burke, M. Ernzerhof, Generalized gradient approximation made simple, Phys. Rev. Lett. 77 (1996) 3865–3868.

[44] J.P. Perdew, Y. Wang, Accurate and simple analytic representation of the electron-gas correlation energy, Phys. Rev. B 45 (1992) 13244–13249.

[45] V.I. Anisimov, J. Zaanen, O.K. Andersen, Band theory and mott insulators: hubbard U instead of stoner I, Phys. Rev. B 44 (1991) 943–954.

[46] H.J. Monkhorst, J.D. Pack, Special points for brillouin-zone integrations, Phys. Rev. B 13 (1976) 5188–5192.

[47] Y.G. Denisenko, N.A. Khritokhin, O.V. Andreev, S.A. Basova, E.I. Sal'nikova, A.A. Polkovnikov, Thermal decomposition of europium sulfates $Eu_2(SO_4)_3{\cdot}8H_2O$ and $EuSO_4$, J. Solid State Chem. 255 (2017) 219–224.

[48] H.B. Larsen, G. Thorkildsen, D.G. Nicholson, P. Pattison, Thermal induced structural properties of silver (I) sulphate (Ag_2SO_4), Cryst. Res. Technol. 51 (2016) 730–737.

[49] A.E. Sedykh, D.G. Kurth, K. Müller-Buschbaum, Two series of lanthanide coordination polymers and complexes with 4′-phenylterpyridine and their luminescence properties, Eur. J. Inorg. Chem. 2019 (2019) 4564–4571.

[50] A.E. Sedykh, S.A. Sotnik, D.G. Kurth, D.M. Volochnyuk, S.V. Kolotilov, K. Müller-Buschbaum, Similarities of coordination polymer and dimeric complex of europium(III) with joint and separate terpyridine and benzoate, Z. Anorg. Allg. Chem. (2020), https://doi.org/10.1002/zaac.201900319.

[51] E.A. Mikhalyova, M. Zeller, J.P. Jasinski, R.J. Butcher, L.M. Carrella, A.E. Sedykh, K.S. Gavrilenko, S.S. Smola, M. Frasso, S.C. Cazorla, K. Perera, A. Shi, H.G. Ranjbar, C. Smith, A. Deac, Y. Liu, S.M. McGee, V.P. Dotsenko, M.U. Kumke, K. Müller-Buschbaum, E. Rentschler, A.W. Addison, V.V. Pavlishchuk, Combination of single-molecule magnet behaviour and luminescence properties in a new series of lanthanide complexes with tris(pyrazolyl)borate and oligo(β-diketonate) ligands, Dalton Trans. 49 (2020) 7774–7789.

[52] K. Lunstroot, L. Baeten, P. Nockemann, J. Martens, P. Verlooy, X. Ye, C. Görller-Walrand, K. Binnemans, K. Driesen, Luminescence of $LaF_3{:}ln^{3+}$ nanocrystal dispersions in ionic liquids, J. Phys. Chem. C 113 (2009) 13532–13538.

[53] H.-R. Mürner, E. Chassat, R.P. Thummel, J.-C.G. Bünzli, Strong enhancement of the lanthanide-centred luminescence in complexes with 4-alkylated 2,2′;6′,2″-terpyridines, J. Chem. Soc., Dalton Trans. (2000) 2809–2816.

[54] R.A. Sá Ferreira, S.S. Nobre, C.M. Granadeiro, H.I.S. Nogueira, L.D. Carlos, O.L. Malta, A theoretical interpretation of the abnormal $^5D_0 \rightarrow {}^7F_4$ intensity based on the Eu^{3+} local coordination in the $Na_9[EuW_{10}O_{36}]{\cdot}14H_2O$ polyoxometalate, J. Lumin. 121 (2006) 561–567.